



The IASI Flux and Temperature project

Valentine Jacquet¹, Sarah Safieddine¹, Maya George¹, Simon Whitburn², Lieven Clarisse², and Cathy Clerbaux^{1,2}

¹ LATMOS/IPSL, Sorbonne Université, UVSQ, CNRS, Paris, France

² Spectroscopy, Quantum Chemistry and Atmospheric Remote Sensing (SQUARES), Université libre de Bruxelles (ULB), Brussels, Belgium



Introduction

The IASI – Flux and Temperature (IASI-FT) project aims to provide new benchmarks for top-of-atmosphere radiative flux and temperature observations using the calibrated radiances measured twice a day at any location by IASI (Clerbaux et al., 2009)¹. This project develops innovative algorithms and statistical tools to generate global climate data records at the global scale of spectrally resolved outgoing radiances, land and sea surface temperatures, and temperatures at selected altitudes. IASI-FT project has received funding from the European Research Council (ERC) under the European Union's Horizon 2020 and innovation programme (grant agreement No 742909).

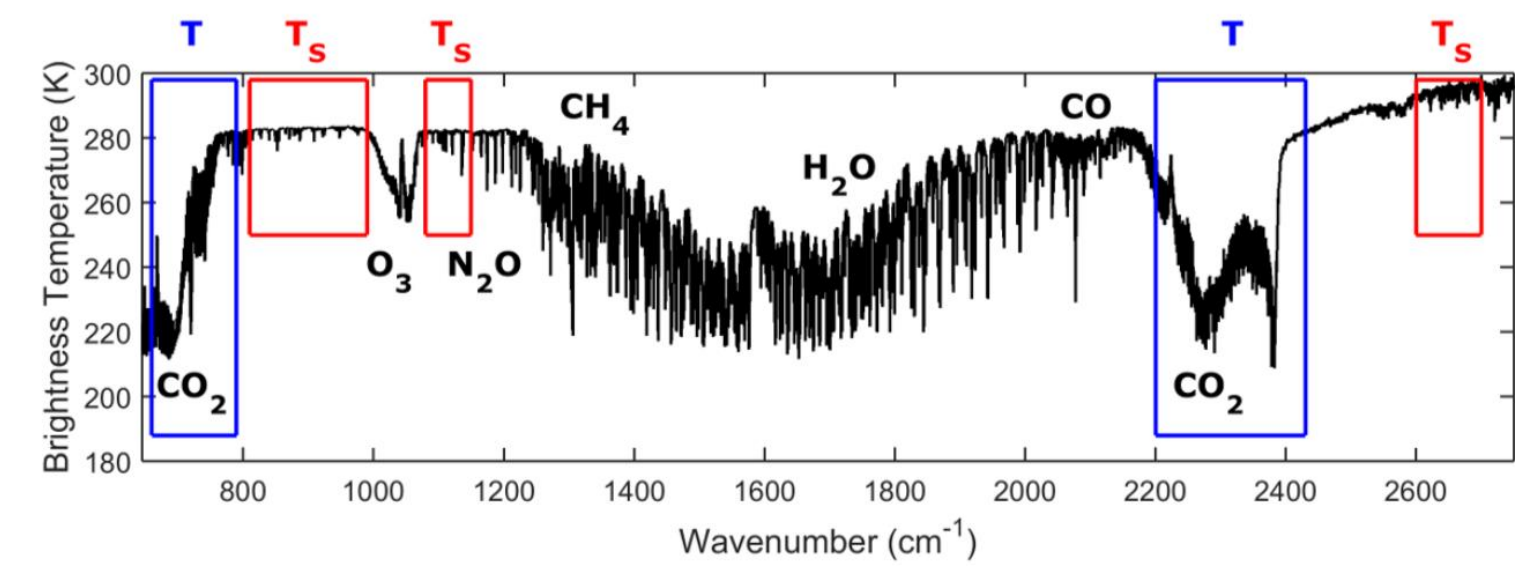


Fig.1 One IASI atmospheric spectrum (in brightness temperature units, normalized with Planck's function). The spectral windows to retrieved skin temperature (T_s , red), and temperature profile (T , blue) and the main molecular absorption features are indicated.

Five products are developed within the IASI-FT project: IASI Outgoing Longwave Radiation, IASI Cloud Detection, IASI Skin Temperature, IASI Sea Surface Temperature, and IASI Atmospheric Temperature Profiles.

- The IASI spectrally resolved Outgoing Longwave Radiation product (IASI OLR)² is a monthly (L3), $2^\circ \times 2^\circ$ global dataset of spectral OLR derived from the clear-sky IASI satellite radiance measurements in the range $645\text{--}2300\text{ cm}^{-1}$ at the 0.25 cm^{-1} native spectral sampling of the L1C spectra. The algorithm for the conversion of the spectra to the OLR is detailed in Whitburn et al. (2020)³.
- The IASI Cloud Detection product (IASI CLD)⁴ is a cloud mask available at the IASI pixel level (L2) that was developed for climate applications purposes. The algorithm is detailed in Whitburn et al. (2022)⁵. It combines an high sensitivity to cloud detection, a very good consistency over time and between the three IASI instruments and simplicity in its parametrization.
- IASI Skin Temperature product (SkT)⁶ is a daily (L2) and a monthly (L3), $1^\circ \times 1^\circ$ global dataset of skin temperatures derived from the IASI satellite radiances data. The data was computed using artificial neural networks over a selected set of IASI radiance channels, trained with ERA5-skin temperature product. Emissivity is also used as input in the neural network (Safieddine et al., 2020)⁷. This method was applied to

the whole IASI time series to produce a homogeneous skin temperature data record from Sept. 2007 to the present (Fig.2). Timeseries and quicklooks plots of T_{skin} anomalies (Fig.3) anomalies are also computed.

- IASI Sea Surface Temperature product (SST)⁸ is a monthly (L3), $1^\circ \times 1^\circ$ global dataset of skin temperatures over the sea derived from the IASI satellite radiances data (Fig.4). The data was computed using Planck's law and simple atmospheric corrections (Parracho et al., 2021)⁹. Timeseries and quicklooks plots of SST anomalies are also computed.
- IASI Atmospheric Temperature Profiles product (ATP)¹⁰ is a daily $1^\circ \times 1^\circ$ global dataset of atmospheric temperatures derived from all IASI radiance observations. The temperatures profiles are given on 11 static pressure levels from 750 to 2 hPa. The method used to retrieve atmospheric temperatures from IASI radiances is detailed in Bouillon et al., 2021¹¹. An Artificial Neural Network (ANN) was applied to reprocessed IASI L1C data, in order to produce a homogeneous atmospheric temperature record from 2008 to present.

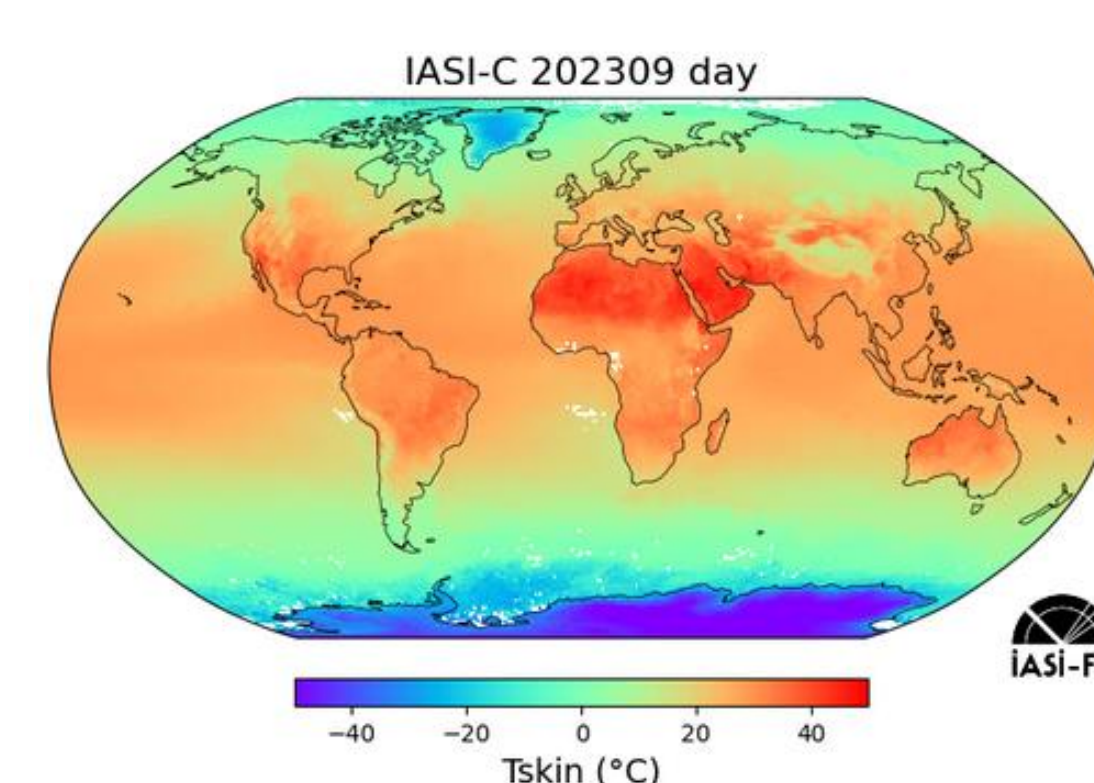


Fig.2 Example of IASI T_{skin} map

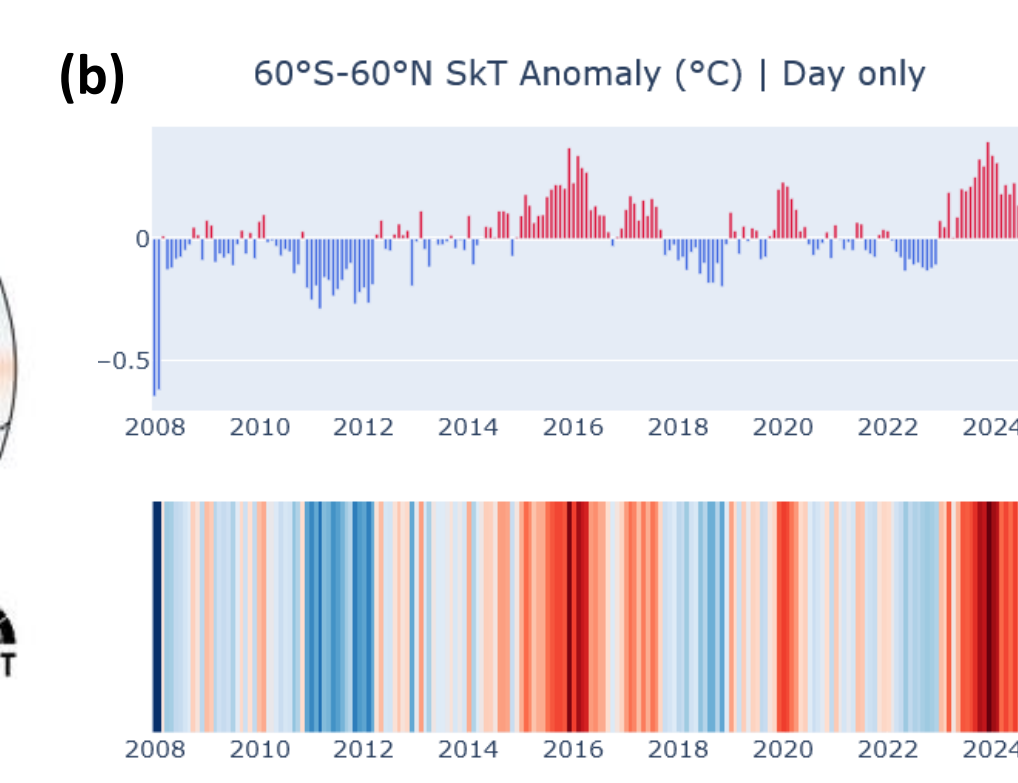
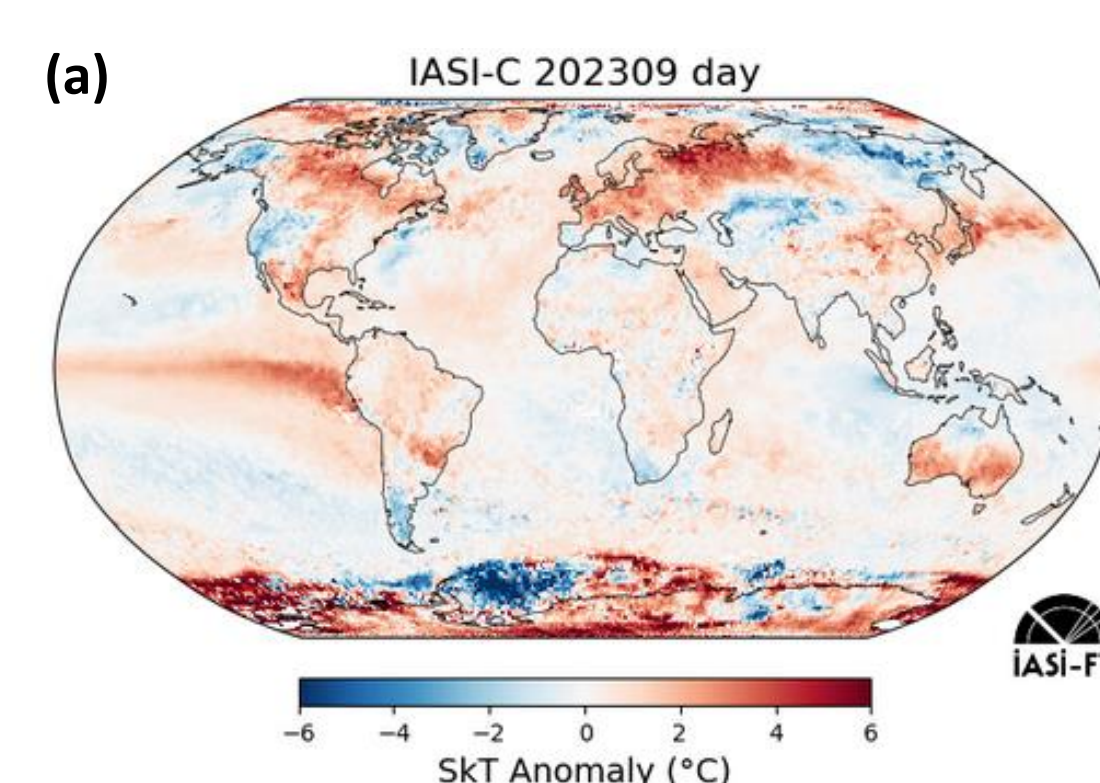


Fig.3 Examples of IASI T_{skin} Anomaly map (a) and quicklooks (b)

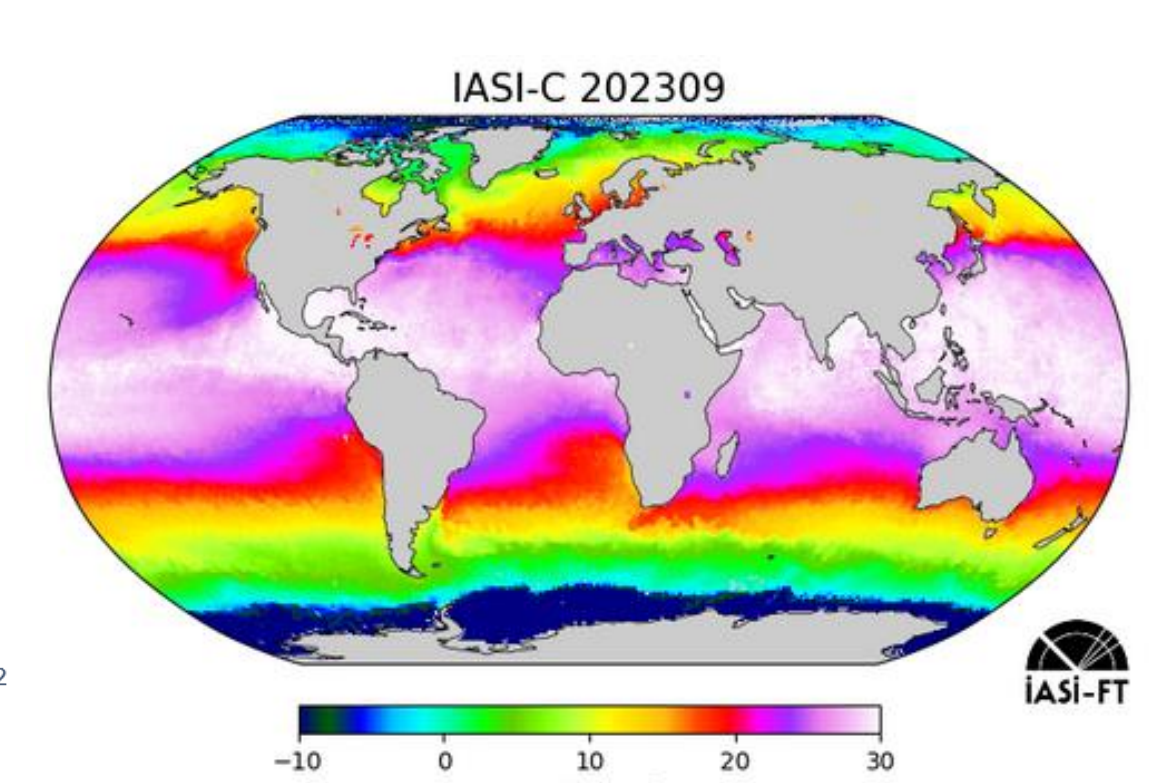


Fig.4 Example of IASI SST map

Available data and figures via www.iasi-ft.eu

Fig.5 Summer 2023 (June, July, August) has been recognized as the warmest summer on record, higher than the previous record in 2016. Extreme events like heatwaves hit some regions, including Europe.

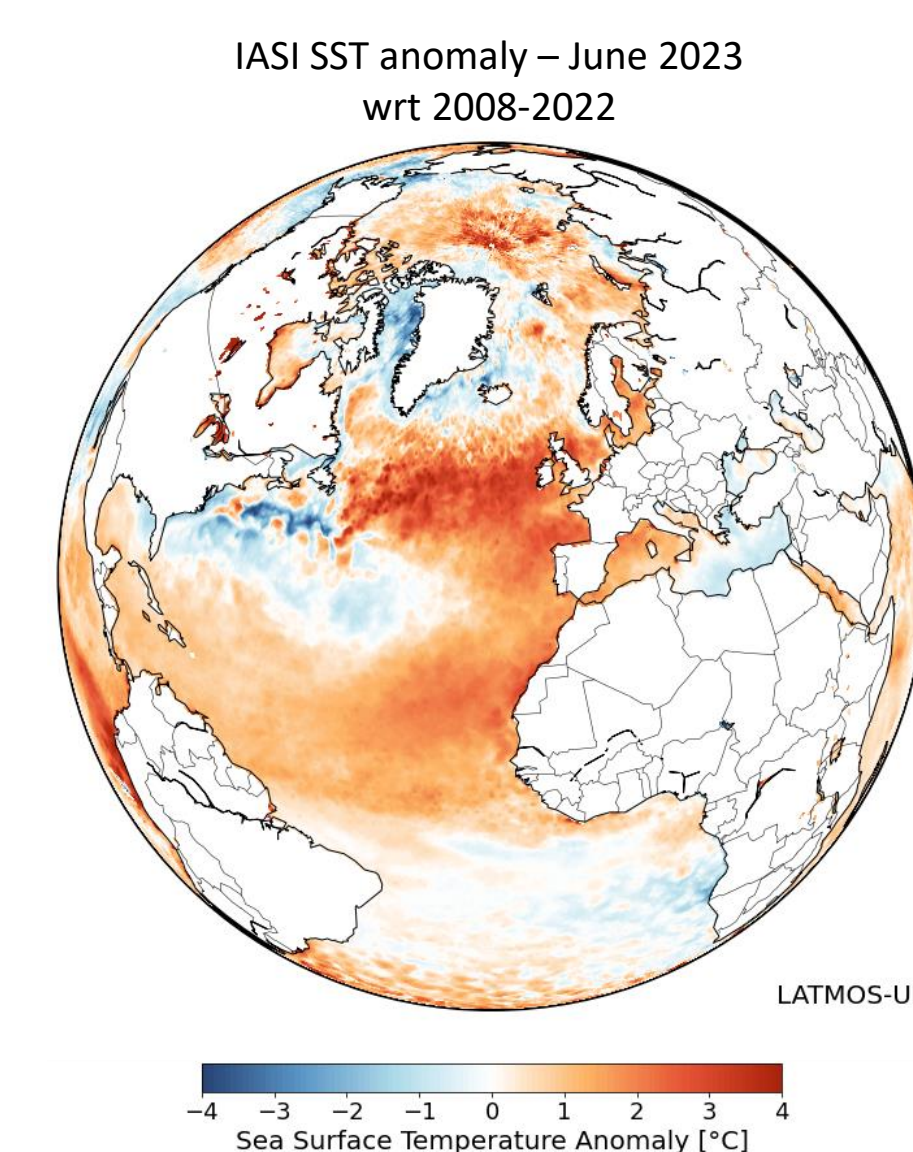
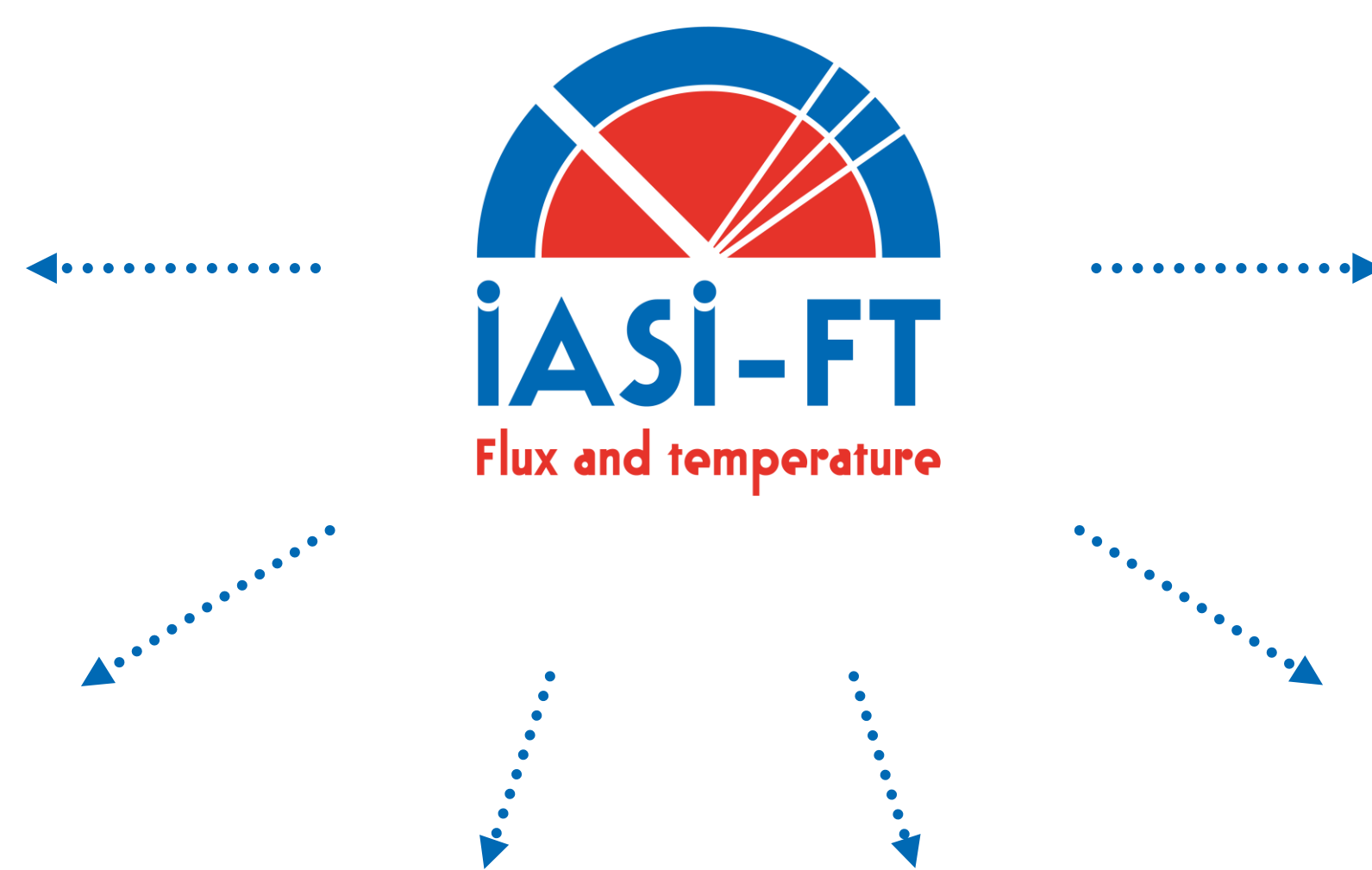
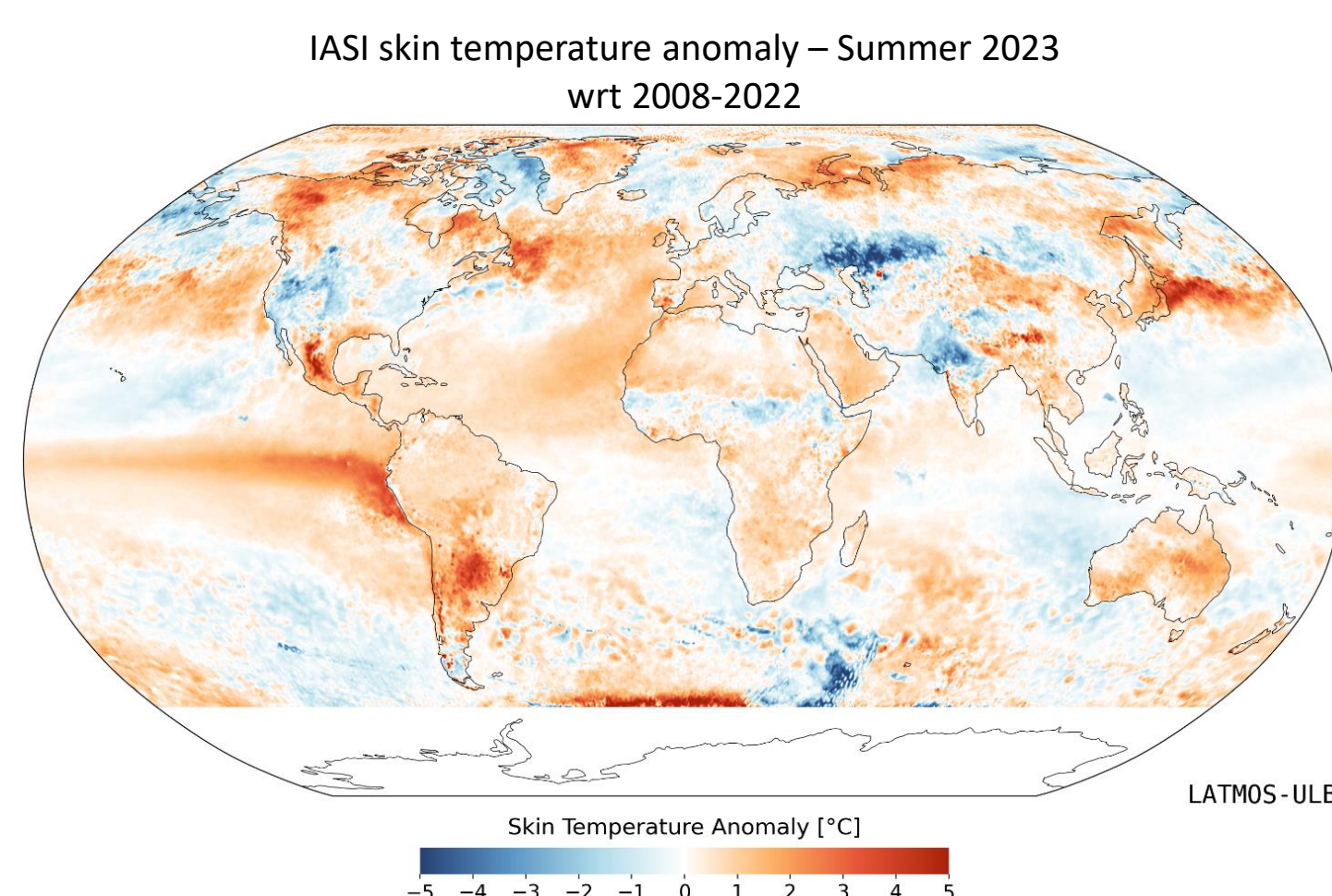


Fig.6 The entire year of 2023 has been exceptional in terms of sea surface temperature. June 2023 in the North Atlantic Ocean recorded the highest temperatures ever for the month of June.

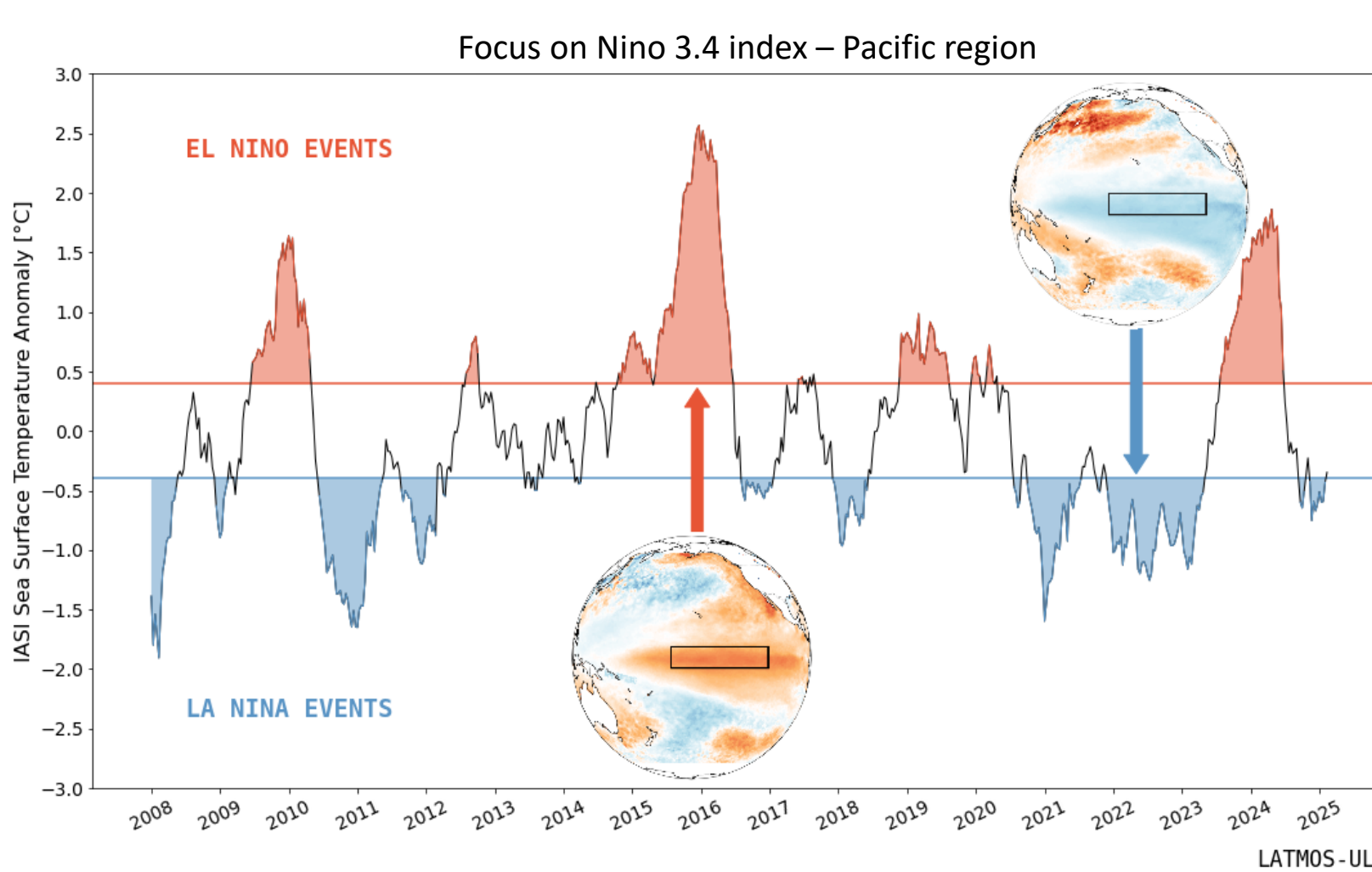


Fig.7 SST anomalies are used to calculate the Niño 3.4 index, in Equatorial Pacific region [5°S – 5°N , 170°W – 120°W]. El Niño or La Niña events are defined as the Niño 3.4 SSTs exceeding $\pm 0.4^\circ\text{C}$ for a period of six months or more. Starting in May 2023 and definitively ending in April 2024, the last El Niño event was one of the biggest episodes observed since the one of 2015–2016.

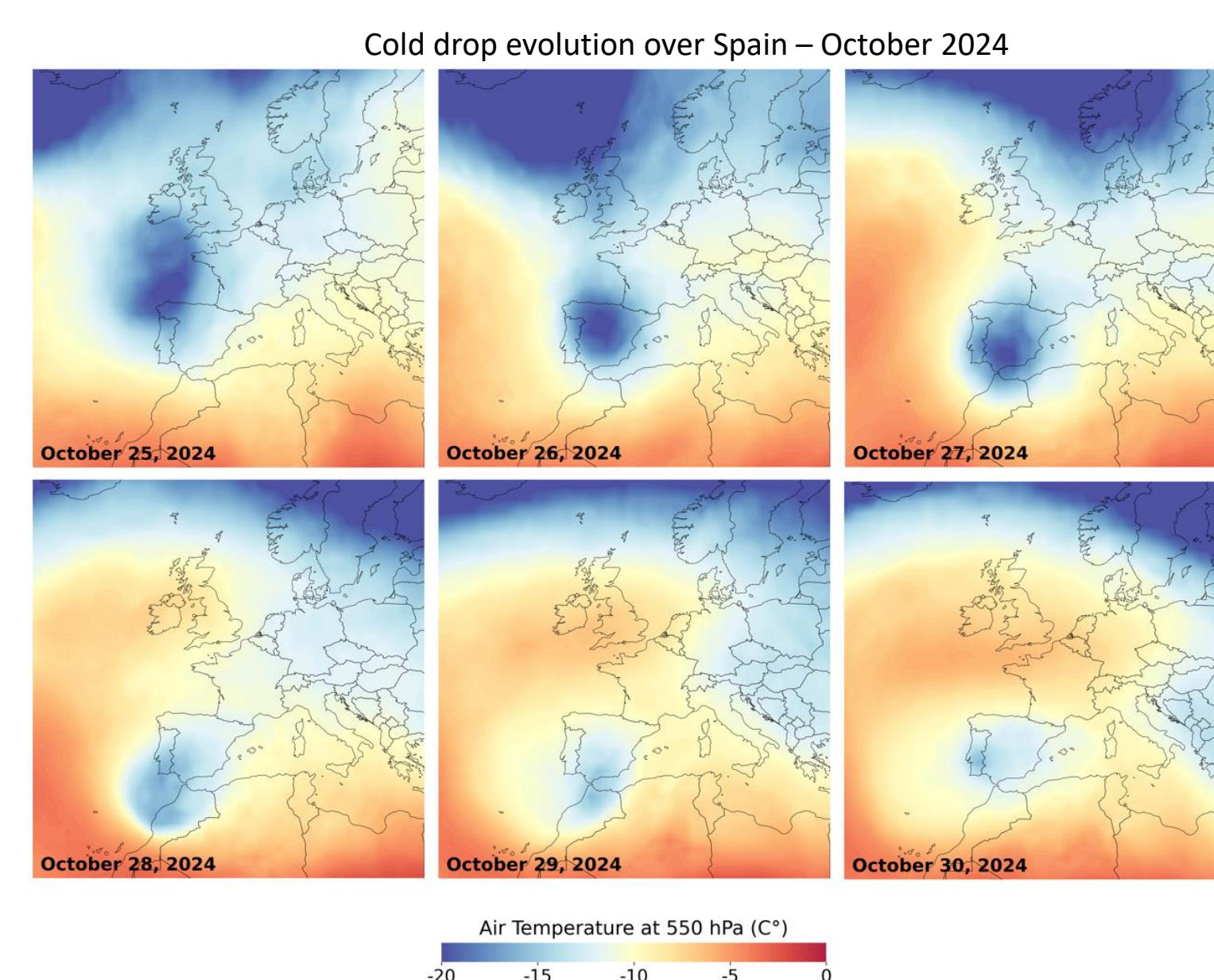


Fig.8 An isolated depression at high altitudes, called cold drop, led to torrential rainfalls event and devastating flash floods in Spain during the night of 29–30 October 2024. This episode was the most intense of the century in the region.

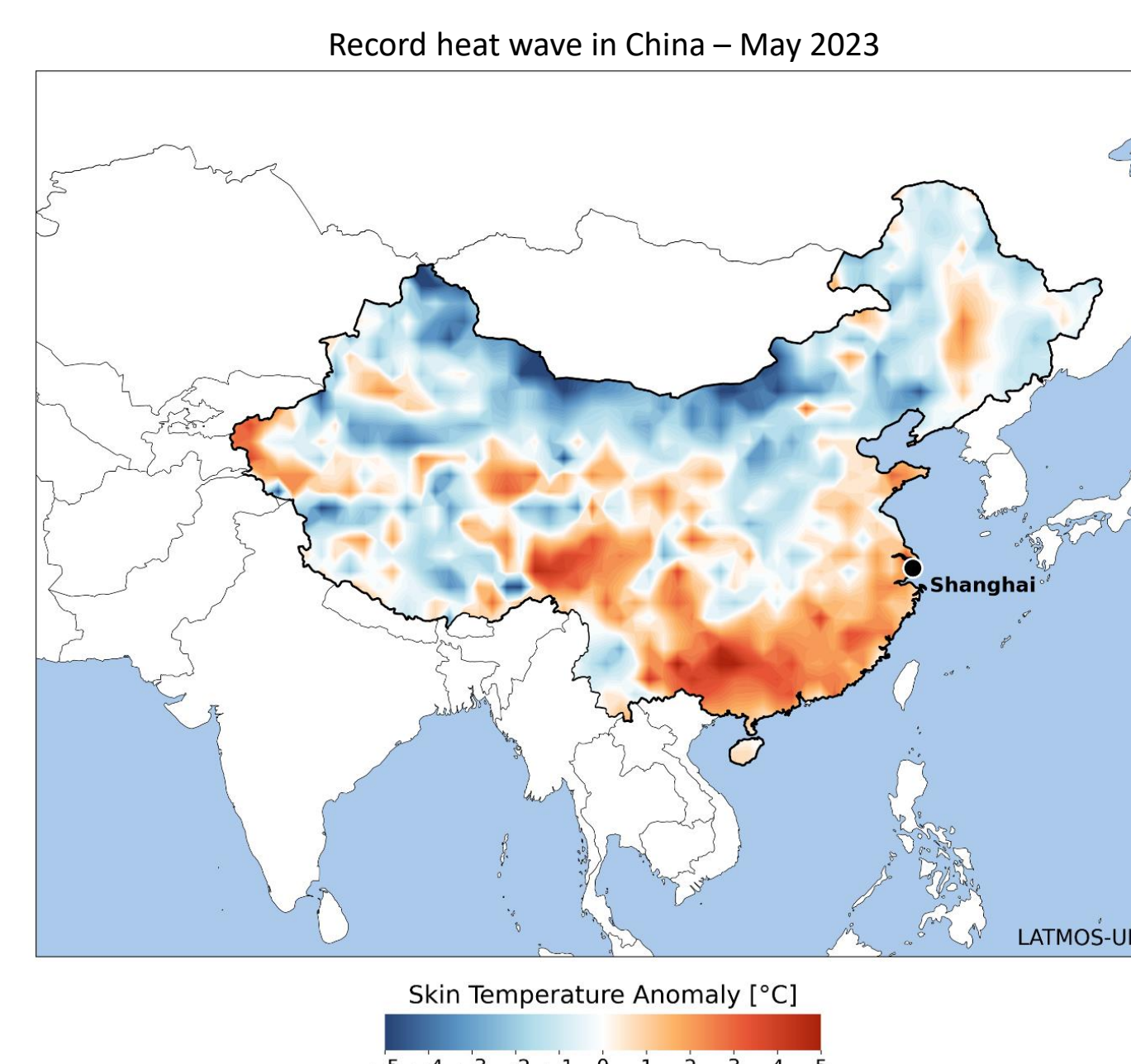


Fig.9 A significant heat wave affected several regions in China during May 2023, with temperature records observed in towns like Shanghai. The red areas indicate skin temperatures exceeding the reference skin temperature for May (wrt 2008-2022).

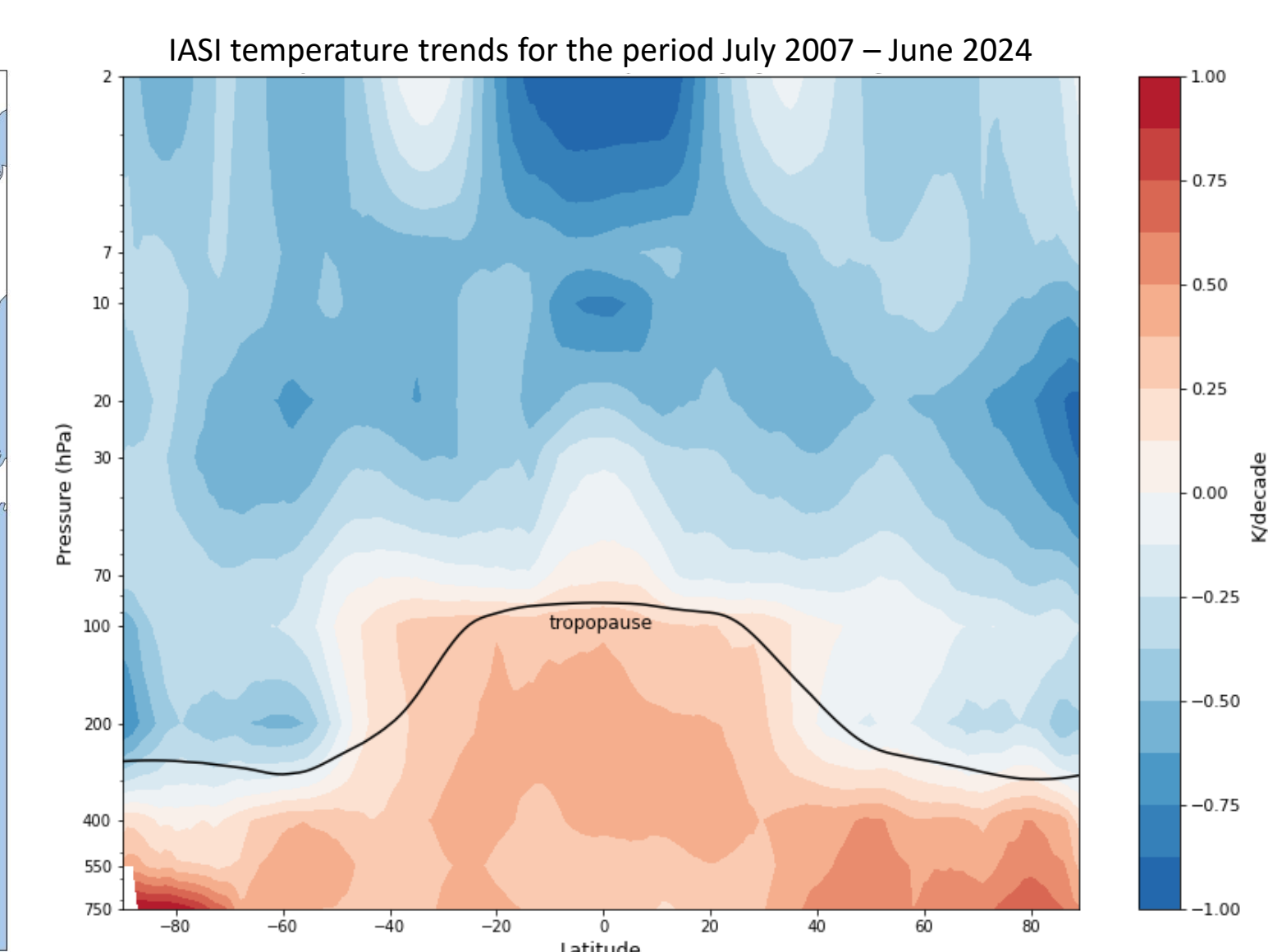


Fig.10 Zonal temperature trends for the period July 2007 – June 2024 computed with the outputs of an Artificial Neural Network (ANN). A general warming of the troposphere, more important at the poles and mid-latitudes, is visible, whereas the stratosphere is globally cooling.

References

- Clerbaux, C. et al.: Monitoring of atmospheric composition using the thermal infrared IASI/MetOp sounder, Atmos. Chem. Phys., 9, 6041–6054, <https://doi.org/10.5194/acp-9-6041-2009>, 2009.
- Whitburn, S. (2021). IASI-FT. Spectrally resolved Outgoing Longwave Radiation (from IASI/MetOp-A, B and C) [Data set]. ULB/LATMOS.
- Whitburn, S. et al.: Spectrally Resolved Fluxes from IASI Data: Retrieval algorithm for Clear-Sky Measurements, <https://doi.org/10.1175/JCLI-D-19-0523.1>, 2020.
- Whitburn, S. (2022). A CO2-free cloud mask from IASI radiances for climate applications (from IASI/MetOp-A, B and C) [Data set]. ULB/LATMOS.
- Whitburn, S. et al.: A CO2-independent cloud mask from Infrared Atmospheric Sounding Interferometer (IASI) radiances for climate applications, <https://doi.org/10.5194/amt-15-6653-2022>, 2022.
- Safieddine, S. (2020). IASI-FT. Skin Temperature (from IASI/MetOp-A, B and C) [Data set]. LATMOS.
- Safieddine, S. et al.: Artificial Neural Networks to retrieve land and sea skin temperature from IASI, Remote Sensing, <https://doi.org/10.3390/rs12172777>, 2020.
- Parracho, A.C., & Safieddine, S. (2021). IASI-FT Sea Surface Temperature (from IASI/MetOp-A, B and C) [Data set]. LATMOS
- Parracho, A.C. et al.: IASI-derived sea surface temperature data set for climate studies, <http://dx.doi.org/10.1029/2020EA001427>, 2021.
- Bouillon, M. (2021). IASI-FT Atmospheric Temperature Profiles [Data set]. LATMOS/ULB.
- Bouillon, M. et al.: Time evolution of temperature profiles retrieved from 13 years of infrared atmospheric sounding interferometer (IASI) data using an artificial neural network, <https://doi.org/10.5194/amt-15-1779-2022>, 2022.